Sensor Fault Detection and Identification in an Electro-pump System using Extended Kalman Filter

Monir Rezaee[1], Nargess Sadeghzadeh-Nokhodberiz[2*], Javad Poshtan[3]
1- Department of Electrical Engineering, Iran University of Science and Technology, Tehran, Iran.
Email:rezaee_monir@yahoo.com
2- Department of Electrical and Computer Engineering, Qom University of Technology, Qom, Iran.
Email:sadeghzadeh@qut.ac.ir (Corresponding author)
3- Department of Electrical Engineering, Iran University of Science and Technology, Tehran, Iran.
Email:jposhtan@iust.ac.ir

Received: September 2020 Revised: January 2021 Accepted: March 2021

ABSTRACT
In this article, the issue of sensor fault detection and identification with sensory information is considered. This is due to the dependence of successful Fult Detection (FD) method on correct sensory measurements that suffer from various soft sensory faults such as bias, drift, scaling factor, and hard faults that can be detected independently. They are not detectable but can be combined with other sensors. To solve this issue, firstly, a state space model for pump subsystem was constructed using the electrical simulation method. Then, the sensory soft faults are modeled and amplified to electro-pump state space model. Both system states and amplified sensory soft faults are then estimated using an Extended Kalman filter (EKF) in which nonlinear model of the induction motor is linearized around the estimated states. Information of current, angular velocity (encoder) and pressure sensors are melted for this goal. The efficiency of the method is firstly evaluated through simulation and then experimental results are provided from our laboratory setup. Measured volume currents, flow, and pressure are compared with simulated signals, and results show that the proposed model is able to successfully describe the laboratory system with good precision. These results show that the model can describe the electro-pump dynamic with good precision.

KEYWORDS: Electro-Pump System, Fault Detection, Sensory Soft Fault, Extended Kalman Filtering.

1. INTRODUCTION

Pumps are important part in a wide range of mechanical operations, such as power plants, the chemical industry, air conditioning, cooling and heating systems, and more. They are commonly used for a variety of industries and used for fluid delivery [1]. Most of them are driven by induction motors, which call the whole system an electro-pump system. Induction motors use robustness, reliability, efficiency and controllability. For electric pumps, proper operation through real-time fault detection and fault reset is essential, as it can be used in a variety of industries, especially the process industry [2].

The idea of conclusive repetition has recently received a great deal of attention in the diagnostic literature compared to hardware redundancy because of its benefits. Approaches to analytical error (FD) detection can be roughly divided into two main classes of models and knowledge-based methods. The first examples use a quantitative analytical model of the physical system, while the second models let the use of qualitative models based on the available information and knowledge of a physical system. If an almost exact mathematical model is available, model-based methods are preferred. This is because these approaches provide more accurate results and are more suitable for performance analysis. Observer-based methods are among the model-based models with wide applications in the framework of modern control theory [3]. Therefore, in this article, observation-based individuals are used.

Faults in an electro-pump are probably due to the pump, motor elements, actuators or sensors. Short-circuit in stator windings is the most common fault in induction motors which devotes 38% of all induction motor failures to itself. The early diagnosis of this fault is of great importance due to the increase of eddy current and the loss of windings insulation. Therefore, different methods which are model-based [4], signal processing-based [5] and intelligent methods [6] have been widely used in diagnosing this fault [7]. However, the main faults in pumps are associated with impeller

Paper type: Research paper
DOI: https://doi.org/10.52547/mjee.15.4.13
How to cite this paper: M. Rezaee, N. Sadeghzadeh-Nokhodberiz and J. Poshtan, **"Sensor Fault Detection and Identification in an Electro-pump System using Extended Kalman Filter"**,Majlesi Journal of Electrical Engineering, Vol. 15, No. 4, pp. 13-25, 2021.

damages [8], rotor faults, seals faults, cavitation [9] and bearing faults. These faults may reduce pump performance or even may cause total failure of the pump system. The overall reliability and safety of many systems rely on the working quality of the pump. Thus, the monitoring and fault diagnosis of pumps plays a key role in maintenance procedures [10].

However, the success of an FD method of all of the above faults is highly dependent on accurate sensory measurements that may suffer from various soft sensory faults such as bias, drift, scaling factor, and hard faults. Detection of these sensory defects in an independent use is completely impractical. Satisfactory performance is immensely reliant on the faithful working of all of its major components of which sensors are the integral part [11].

The literature on current sensors FDI shows a variety of approaches based on hardware redundancy, software redundancy, or both of them [12]. Efficient sensory defect detection is usually performed by sensor fusion [13]. In particular, defects in sensors can lead to major consequences for the performance of industrial devices. As shown in [14], a fault in a current sensor can cause an overcurrent in the induction motor in a short period of time in which the overcurrent protection method must be used. In addition, mechanical speed or position sensors are more prone to error than current sensors. However, they affect the phase current almost after a long time, which makes the error detection method unrealistic in time [14]. In this regard, the design of FD methods for mechanical sensors with promising results has been widely considered in the literature [15], [16] however, the current FD of sensors still needs to be examined.

Most diagnostic methods in the literature are based on hardware redundancy [17], [18]. However, the use of redundant sensors increases the size and cost of the system [19]. For this reason, some research studies suggest FD methods using only two-sensor information. For example, in [20], a compatible observer is proposed to detect faults in current, speed or voltage sensors. This method is based on the assumption that there is probably only one faulty sensor at a time, meaning that only single faults can be separated. This method requires calculating the average residual value.

A similar method for Fault Detection and Isolation (FDI) single-sensor faults has been reported in [19]. The FDI is performed by calculating Kalman filter residues (KF) and absolute values of currents. These residues are not completely separated from each other, so the thresholds must be carefully selected with the experimental algorithms proposed in the paper. This method is not able to detect the recovery of a sensor from a defective situation, for example, after a short-term fault [21].

In this paper, however, similar to [22] sensory soft faults (biases, drifts, and scaling factors) are modeled and augmented to system state parameters in our electro-pump application. Using its electrical analogy, a mathematical model for pump subsystem is created to provide a suitable model which is correlated with sensor measurements. Then, an EKF (extended Kalman filtering) method is employed to estimate system states and the extent of sensory soft faults fusing the information of current, angular velocity (encoder) and pressure sensors.

In this article, similar to [19], soft sensory faults (biases, drifts and scaling factors) are modeled and amplified in the application of our electro pump to the system state parameters. Using its electrical analogy, a mathematical model is created for the pump subsystem to provide a suitable model that correlates with sensor measurements. Then, an EKF (extended Kalman filtering) method is used to estimate the state of the system and the amount of soft sensory faults using the information of flow, angular velocity (encoder) and pressure sensors.

The rest of this article is as follows: Some information about system and sensor error models is provided in Section 2. The EKF is then reviewed and used in Section 3. The simulation results are presented in Section 4 to show the efficiency of the proposed method. In Section 5, this method is evaluated through the experimental results obtained from the operation of the laboratory. Ultimately, a summary is available in Section 6.

2. SYSTEM MODELING AND PROBLEM FORMULATION AND FAULTS

In this section, firstly, nonlinear model of the induction motor is presented. Then, a mathematical model for pump subsystem is proposed using its electrical analogy.

2.1. Nonlinear Dynamic Model of an Induction Motor

The induction motor model is described in two stationary reference frames, denoted by (α,β). This frame is obtained by linear transformations applied to the three-phase electromagnetic variables, denoted by (a,b,c). A graphic representation of the stationary reference frame is shown in Fig. 1, where ζ denotes the components of the currents, voltages or fluxes. It can be observed that in the (α,β) frame, the α component is aligned with axis a. In order to obtain the representation of the induction motor model in the (α,β) frame, the following transformation is employed:

$$\begin{bmatrix}\xi_\alpha & \xi_\beta\end{bmatrix}^T = T\begin{bmatrix}\xi_a & \xi_b & \xi_c\end{bmatrix}^T \quad (1)$$

where,

$$T = \sqrt{\frac{2}{3}}\begin{bmatrix} 1 & -\frac{1}{2} & -\frac{1}{2} \\ 0 & \frac{\sqrt{3}}{2} & -\frac{\sqrt{3}}{2} \end{bmatrix}.$$

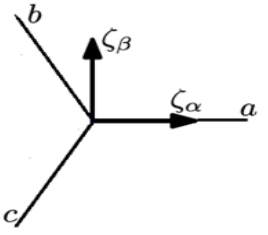

Fig. 1. Graphic representation of the stationary reference frame [21].

The model is represented in the (α, β) frame by the following dynamic equations:

$$\frac{di_\alpha}{dt} = -ai_\alpha + bc\lambda_\alpha + b\omega\lambda_\beta + dv_\alpha \quad (2.1)$$

$$\frac{di_\beta}{dt} = -ai_\beta + bc\lambda_\beta - b\omega\lambda_\beta + dv_\beta \quad (2.2)$$

$$\frac{d\lambda_\alpha}{dt} = L_M ci_\alpha - c\lambda_\alpha - \omega\lambda_\beta \quad (2.3)$$

$$\frac{d\lambda_\beta}{dt} = L_M ci_\beta - c\lambda_\beta + \omega\lambda_\alpha \quad (2.4)$$

$$\frac{d\omega}{dt} = -kc_f\omega + kc_t(i_\alpha\lambda_\beta - i_\beta\lambda_\alpha) - kT_L \quad (2.5)$$

Where, i_α and i_β are stator currents; λ_α and λ_β are rotor fluxes; ω is the rotor speed; v_α and v_β are stator voltages; T_L is the load torque. Thus, $X = \begin{bmatrix} i_\alpha & i_\beta & \lambda_\alpha & \lambda_\beta & \omega \end{bmatrix}^T$ is the state vector of induction motor subsystem and v_α, v_β and T_L are considered as arbitrary inputs, and the constants are as follows:

$$a = \frac{L_r^2 R_s + L_M^2 R_r}{\sigma L_r}\ ,\ b = \frac{L_M}{\sigma}\ ,\ c = \frac{R_r}{L_r}\ ,$$

$$d = \frac{L_r}{\sigma} \quad (3\text{–}1)$$

$$\sigma = (L_r L_s - L_M^2)\ ,\ k = 1/J\ ,\ c_t = \frac{pL_M}{L_r} \quad (3\text{–}2)$$

R_s and R_r are stator and rotor resistances, respectively; L_s, L_r and L_M are stator, rotor and magnetizing inductances, respectively; J and p are the moment of inertia and the number of pole pairs, respectively; c_f is the friction coefficient [21].

2.2. Modeling of Pump and Tank by Electrical Analogy Method

In this subsection, we develop a model for hydraulic subsystem including pump and tank components using electrical analogy method. The employed experimental setup is depicted in Fig. 2. The system consists of a 3KW induction motor and a 3-stage centrifugal pump. The schematic of the employed pump and tank system has been depicted in Fig. 3. As it is depicted in the figure, the system is composed of a pump, a reservoir tank and connecting pipes. The length of connecting pipes is represented by l_i, $i = 1,2,3$. Due to the pressure and fluid flow changes in the system, pressure and flow of different parts are represented by P_i, $i = 1,2,3,4$ and q_i, $i = 1,2$, respectively. Besides, h is the tank height.

.

Fig. 2. Electro-pump system in system identification Lab., Iran Univ. of Sci. & tech.

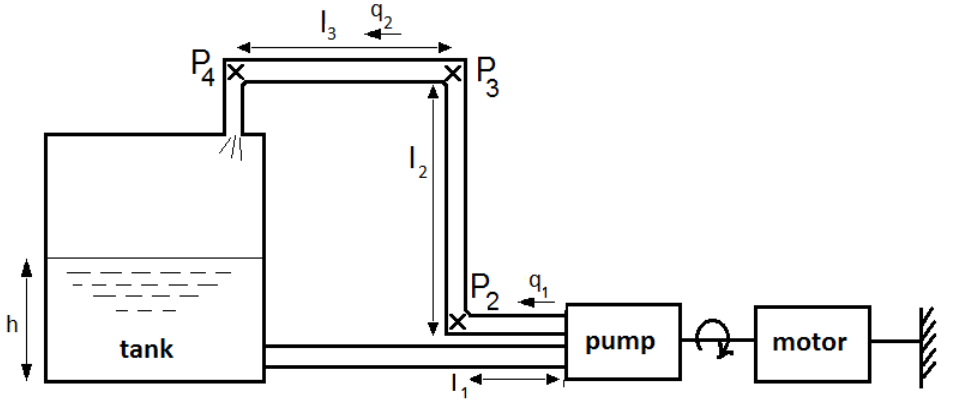

Fig. 3. Graphic representation of pump and tank system.

Now, the electrical analogy method [20] is employed for the hydraulic subsystem. In this method, a reservoir is modeled by a capacitor, a pipe by inductor a cross section change by resistor and a pump by voltage or current source.

- Electrical analogy of hydraulic components:

Reservoir: In the electrical analogy approach, a reservoir is modeled by a capacitor. Consider a reservoir as depicted in Fig 4. The following equations relate the reservoir to the capacitor.

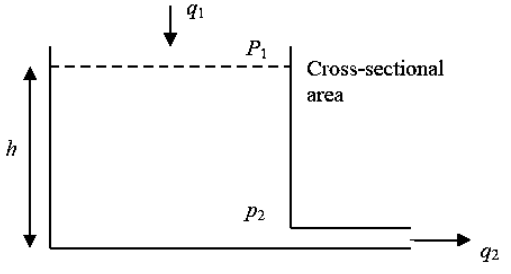

Fig. 4. Scheme of reservoir.

$$q_1 - q_2 = \frac{dV}{dt} \tag{4–1}$$

$$V = Ah \tag{4–2}$$

$$q_1 - q_2 = \frac{V(Ah)}{dt} = A\frac{dh}{dt} \tag{4–3}$$

$$q_1 - q_2 = A\frac{d(p/\rho g)}{dt} = \frac{A}{\rho g}\frac{dp}{dt} \tag{4–4}$$

Where $q_{1,2}$, p, V, h, A, ρ, g are flow, pressure, volume, the cross-section of the tank, liquid density and gravity acceleration constant, respectively.

Thus, the reservoir can be modeled by a capacitor with the following capacity:

$$C = \frac{A}{\rho g} \tag{4–5}$$

Pipe: If a pipeline is long enough, it is modeled by an inductor as an electrical component in the electrical analogy approach. Besides, any change in cross-section of the pipeline is modeled by a resistor. Consider a pipeline as depicted in Fig 5. The following equations show how a pipeline can be related to an inductor through formulas:

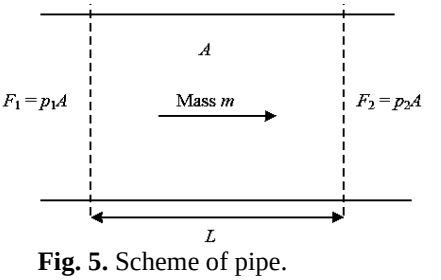

Fig. 5. Scheme of pipe.

$$F_1 - F_2 = p_1A - p_2A = (p_1 - p_2)A = ma \tag{5–1}$$

$$(p_1 - p_2)A = m\frac{dv}{dt} \tag{5–2}$$

$$m = AL\rho, q = Av \tag{5–3}$$

$$(p_1 - p_2)A = AL\rho\frac{dv}{dt} \tag{5–4}$$

$$(p_1 - p_2)A = \frac{L\rho}{A}\frac{dq}{dt} \tag{5–5}$$

Where, A, ρ, L, m, v and a are cross-section of pipes, liquid density, pipe's length, liquid mass, liquid velocity and, liquid acceleration, respectively.

Thus the corresponding inductance of a pipeline is calculated as follows:

$$l = \frac{L\rho}{A} \tag{5–6}$$

Besides, as mentioned earlier, any changes in cross-section of the pipe is modeled by a resistor component in the electrical analogy approach which can be determined by experimental data.

Pump: A pump as a pressure producer in the hydraulic system is modeled by voltage or current source in an electrical system. In this paper, we replace a pump with a voltage source with a constant value of p_s. Electrical analogy modeling of laboratory hydraulic system:

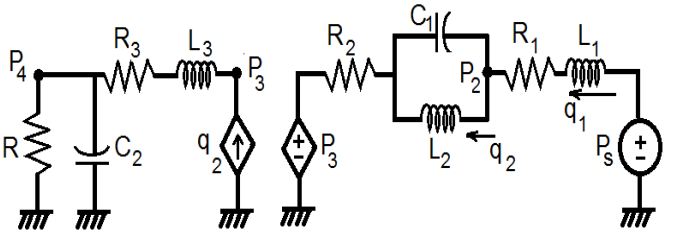

Fig. 6. Electrical model of pump and tank system.

Therefore, the equivalent electrical model as shown in Fig. 6 is obtained from. Analyzing the electrical circuit of Fig. 6, dynamics of the hydraulic subsystem can be described as follow:

$$\frac{dq_1}{dt} = \frac{-(R_1+R_2)}{L_1} q_1 + \frac{R_3+L_2}{L_1 L_3} q_2 - \frac{1}{L_1}(1+\frac{L2}{L3}) p_3 + \frac{L_2}{L_1 L_3} p_4 + \frac{p_s}{L_1} \tag{6–1}$$

$$\frac{dq_2}{dt} = \frac{-R_2}{L_2} q_1 + \frac{1}{L_2} p_2 - \frac{1}{L_2} p_3 \tag{6–2}$$

$$\frac{dp_2}{dt} = (\frac{1}{C_1} + \frac{L_3}{C_1 L_2} - \frac{R_2(R_1+R_2)}{L_2}) q_1 + (-\frac{1}{C_1} + \frac{1}{C_2} - \frac{L_3}{C_1 L_2} + \frac{R_3^2}{L_3} + \frac{R_2 R_3 L_2}{L_1 L_3}) q_2 + (\frac{-R_3}{L_3} - \frac{R_2}{L_1}(1+\frac{L_2}{L_3})) p_3 + (\frac{R_3}{L_3} - \frac{1}{RC_2} + \frac{R_2 L_2}{L_1 L_3}) p_4 + \frac{R_2}{L_1} p_s \tag{6–3}$$

$$\frac{dp_3}{dt} = \frac{L_3}{C_1 L_2} q_1 + (\frac{1}{C_2} - \frac{L_3}{C_1 L_2} + \frac{R_3^2}{L_3}) q_2 - \frac{R_3}{L_3} p_3 + (\frac{R_3}{L_3} - \frac{1}{RC_2}) p_4 \tag{6–4}$$

$$\frac{dp_4}{dt} = \frac{1}{C_2} q_2 - \frac{1}{RC_2} p_4 \tag{6–5}$$

Where p_i, ($i = 1,2,3,4$) and q_i, ($i = 1,2$) are pressure and flux respectively as shown in Fig. 5 and equation (4-5, 5-6 and 6). We assume q_1, q_2, p_2, p_3, p_4 as states and p_s is the output pressure of pump that we assume it constant and as an input.

3. Sensor Fault Modelling and Augmentation

In this section, sensory soft faults (biases, drifts, and scaling factors) are modeled in the form of state space model and then they are augmented to the motor and pump state space models. Finally, a general augmented model is introduced.

3.1. Soft faults in sensors

All type of sensors are disturbed with the following sensory faults which are referred to as soft faults [21], [10]:

- Bias: A constant offset from the nominal sensor signal statistics. It is the sensor output at zero input. Bias can occur due to incorrect calibration physical changes in the sensory system.
- Drift: A time-varying offset from the nominal statistics of the sensor signal.
- Scaling factor: Magnitudes are scaled by a factor where the waveform itself does not change.

Accordingly, a general sensor output model has the following form [20]:

$$S_m = (1+s_f) S_t + b(t) \tag{7}$$

Where, S_m is the sensor's measured output, S_t is the true value of the quantity that the sensor is measuring and is corrupted by the scale factor error s_f and the bias $b(t)$. The bias term, $b(t)$ has the following form:

$$b(t) = b_0 + b_1(t) + n(t) \tag{8}$$

The term b_0 represents constant offset or bias, $b_1(t)$ represents time varying offset or sensor drift, and the term $n(t)$ represents the measurement noise. If the values of the variable s_f and the components of $b(t)$ are identified, the true value of S_t can be extracted from the measurement. They can be computed online using an estimator (in this paper EKF) as a part of state estimation system. It should be mentioned that the value of bias is sometimes listed on the data sheet. The main challenge is to determine $b_1(t)$. To this end, it is crucial to have a model of its time variations. A Gauss–Markov process with an additive wide-band noise η_{b_1}, is introduced as an appropriate model for drift in [23] as follows:

$$\dot{b_1}(t) = -\frac{1}{\tau} b_1(t) + \eta_{b_1} \tag{9}$$

Where, τ is the process time constant [13].

Moreover, since bias and scaling factor are constants, they can be modeled by the following static state space model with additive noises, η_{b_0} and, η_{s_f}, respectively:

$$\dot{b_0}(t) = \eta_{b_0} \tag{10}$$

$$\dot{s_f}(t) = \eta_{s_f} \tag{11}$$

3.1. Current Sensor Soft Fault Modeling and Augmentation to Motor Model

In this subsection, according to the introduced modeling of the soft faults in equations (8)-(12), firstly, the faults in the current sensors are modeled and then they are augmented to the introduced motor model in equations (2) and (3). In our introduced system, we are using three current sensors, one for each phase. After coordinate transformation from (a,b,c) to (α,β), they are mathematically transformed to two current sensors and their corresponding fault models are as follows:

$$S_{m_{i_\alpha}} = (1+s_{f_{i_\alpha}})S_{t_{i_\alpha}} + b_{0_{i_\alpha}} + b_{1_{i_\alpha}}(t) + n_{i_\alpha}(t) \tag{12–1}$$

$$S_{m_{i_\beta}} = (1+s_{f_{i_\beta}})S_{t_{i_\beta}} + b_{0_{i_\beta}} + b_{1_{i_\beta}}(t) + n_{i_\beta}(t) \tag{12–2}$$

$$\dot{b}_{0_{i_\alpha}}(t) = \eta_{b_{0i_\alpha}} \tag{12–3}$$

$$\dot{b}_{0_{i_\beta}}(t) = \eta_{b_{0i_\beta}} \tag{12–4}$$

$$\dot{b}_{1_{i_\alpha}}(t) = -\frac{1}{\tau_{i_\alpha}} b_{1_{i_\alpha}}(t) + \eta_{b_{1i_\alpha}} \tag{12–5}$$

$$\dot{b}_{1_{i_\beta}}(t) = -\frac{1}{\tau_{i_\beta}} b_{1_{i_\beta}}(t) + \eta_{b_{1i_\beta}} \tag{12–6}$$

$$\dot{s}_{f_{i_\alpha}}(t) = \eta_{s_{f_{i_\alpha}}} \tag{12–7}$$

$$\dot{s}_{f_{i_\beta}}(t) = \eta_{s_{f_{i_\beta}}} \tag{12–8}$$

Where, $S_{m_{i_\alpha}}$ and $S_{m_{i_\beta}}$ are the sensor's measured outputs of i_α and i_β. $S_{t_{i_\alpha}}$ and $S_{t_{i_\beta}}$ are the true values of the quantities which are corrupted by the scale factors of $S_{f_{i_\alpha}}$ and $S_{f_{i_\beta}}$, offsets of $b_{0_{i_\alpha}}$ and $b_{0_{i_\beta}}$, drifts of $b_{1_{i_\alpha}}$ and $b_{1_{i_\beta}}$ and noises of n_{i_α} and n_{i_β} which are zero mean Gaussian measurement noises. $\tau_{(.)}$ refers to process time constants and $\eta_{(.)}$ refers to zero mean Gaussian noise. Thus biases, drifts and scaling factors of current sensors are generally modeled as follows:

$$\dot{x}_1(t) = A_1 x_1(t) + \omega_1(t) \tag{13–1}$$

$$y_1 = C_1 x_1(t) + \nu_1(t) \tag{13–2}$$

Where, $x_1 \in {}^{6}$ is system state with the following parameters:

$$x_1 = \begin{bmatrix} b_{0i_\alpha} & b_{1i_\alpha} & s_{fi_\alpha} & b_{0i_\beta} & b_{1i_\beta} & s_{fi_\beta} \end{bmatrix}^T \tag{14}$$

And, $y_1 = [S_{m_{i_\alpha}} \; S_{m_{i_\beta}}]^T \in {}^{2}$ is system output. $\omega(t)$ and $\nu(t)$ are zero mean Gaussian process and measurement noises which are mutually uncorrelated. Besides:

$$A_1 = \mathrm{diag}(0, -1/\tau_{i_1}, 0, 0, -1/\tau_{i_2}, 0) \tag{15}$$

Besides,

$$C_1 = \begin{bmatrix} 1 & 1 & i_\alpha & 0 & 0 & 0 \\ 0 & 0 & 0 & 1 & 1 & i_\beta \end{bmatrix} \tag{16}$$

Now, sensory faults are augmented to the motor model. The motor model is nonlinear and after linearization, the following general continuous time linear model is obtained:

$$\dot{x}_T(t) = A_T x_T(t) + B_T u_T(t) + \omega_T(t) \quad (17\text{–}1)$$

$$y_T = C_T x_T(t) + \nu_T(t) \quad (17\text{–}2)$$

Where, $x_T \in$ ^{11} is system state with the following parameters:

$$x_T = [i_\alpha \quad i_\beta \quad \lambda_\alpha \quad \lambda_\beta \quad \omega \quad b_{0i_\alpha} \quad b_{1i_\alpha} \quad s_{fi_\alpha} \quad b_{0i_\beta} \quad b_{1i_\beta} \quad s_{fi_\beta}]^T \quad (18)$$

$u_T \in$ ^{3} is system input:

$$u_T = [v_\alpha \quad v_\beta \quad T_L]^T \quad (19)$$

And, $y_T \in$ ^{3} is system output which shows the sensor measurements. $\omega_T(t)$ and $\nu_T(t)$ are process and measurement noises which are zero mean Gaussian noises. Moreover:

$$A_T = \begin{bmatrix} A_{11} & 0 \\ 0 & A_{22} \end{bmatrix}_{11\times 11} \quad (20)$$

Where

$$A_{11} = \begin{bmatrix} -a & 0 & bc & b\omega & b\lambda_\beta \\ 0 & -a & -b\omega & bc & -b\lambda_\alpha \\ L_M c & 0 & -c & -\omega & -\lambda_\beta \\ 0 & L_M c & \omega & -c & \lambda_\alpha \\ kc_t\lambda_\beta & -kc_t\lambda_\alpha & -kc_t i_\beta & kc_t i_\alpha & kc_f \end{bmatrix}$$

and $A_{22} = A_1$ is defined in Equation (15) and other parameters are introduced in Equations (2) and (3). Moreover:

$$B_T = \begin{bmatrix} B_{11} \\ B_{21} \end{bmatrix}_{11\times 3} \quad (21)$$

Where

$$B_{11} = \begin{bmatrix} d & 0 & 0 \\ 0 & d & 0 \\ 0 & 0 & 0 \\ 0 & 0 & 0 \\ 0 & 0 & -k \end{bmatrix}, \quad B_{21} = [0]_{6\times 3}$$

Where d, k are constants as presented previously. Besides:

$$C_T = \begin{bmatrix} 1 & 0 & 0 & 0 & 0 & 1 & 1 & i_\alpha & 0 & 0 & 0 \\ 0 & 1 & 0 & 0 & 0 & 0 & 0 & 0 & 1 & 1 & i_\beta \\ 0 & 0 & 0 & 0 & 1 & 0 & 0 & 0 & 0 & 0 & 0 \end{bmatrix} \quad (22)$$

Discretizing the state space model, the following is obtained:

$$x_{T,k+1} = \varphi_T x_{T,k} + \Gamma_T u_T(k) + \omega_{T,k} \quad (32)$$

Where $x_{T,k}$ is the state vector of the process at time instant k, φ_T is the state transition matrix of the process from the state at k k to state at $k+1$, $\omega_{T,k}$ is the associated discrete zero mean white Gaussian noise with the known covariance matrix of $Q_T = E[\omega_{T,k}\omega_{T,k}{}^T]$. Observations on this variable can be modeled in the form;

$$y_{T,k} = H_T x_{T,k} + \nu_{T,k} \quad (24)$$

Where; $y_{T,k}$ is the sensor measurement model H_T is the measurement vector, $\nu_{T,k}$ is the discrete measurement zero mean white Gaussian noise with the known covariance matrix of $R_T = E[\nu_{T,k}\nu_{T,k}{}^T]$. This is again assumed to be a white noise process with known covariance and has zero cross-correlation with the process noise.

3.2. Flow and Pressure Sensors Soft Fault Modeling and Augmentation to Pump Model

In this subsection, according to the introduced modeling of the soft faults in equations (8)-(12), firstly, the faults in pressure and flow sensors are modeled and then they are augmented to the pump model in equations (7). Faulty model for pressure and flow sensors are presented as follow:

$$S_{m_{q_2}} = (1 + s_{f_{q_2}})S_{t_{q_2}} + b_{0_{q_2}} + b_{1_{q_2}}(t) + n_{q_2}(t) \quad (25\text{–}1)$$

$$S_{m_{p3}} = (1+s_{f_{p3}})S_{t_{p3}} + b_{0_{p3}} + b_{1_{p3}}(t) + n_{p_3}(t) \quad (25\text{–}2)$$

$$\dot{b}_{0_{q_2}}(t) = \eta_{b_{0q_2}} \quad (25\text{–}3)$$

$$\dot{b}_{0_{p_3}}(t) = \eta_{b_{0p_3}} \quad (25\text{–}4)$$

$$\dot{b}_{1q_2}(t) = -\frac{1}{\tau_{q_2}} b_{1_{q_2}}(t) + \eta_{b_{1q_2}} \quad (26\text{–}5$$

$$\dot{b}_{1_{p_3}}(t) = -\frac{1}{\tau_{p_3}} b_{1_{p_3}}(t) + \eta_{b_{1p_3}} \quad (25\text{–}6)$$

$$\dot{s}_{f_{q_2}}(t) = \eta_{s_{f_{q2}}} \quad (25\text{–}7)$$

$$\dot{s}_{f_{p3}}(t) = \eta_{s_{f_{p3}}} \quad (25\text{–}8)$$

Where $S_{m_{q_2}}$ and $S_{m_{p3}}$ are the measured values of flow and pressure according to Fig. 3. $S_{t_{q2}}$ and $S_{t_{p3}}$ are the true values of the quantities which are corrupted by the scaling factors of $S_{f_{q2}}$ and $S_{f_{p3}}$, biases of $b_{0_{q2}}$ and $b_{0_{p3}}$, time-varying drifts of $b_{1_{q_2}}$ and $b_{1_{p3}}$ and noises of n_{q_2} and n_{p_3} which are zero mean Gaussian measurement noises. $\tau_{(.)}$ represent process time constants, $\eta_{(.)}$ refer to additive zero mean Gaussian noises.

Thus biases, drifts and scaling factors are modeled as follows:

$$\dot{x}_2(t) = A_2 x_2(t) + \omega_2(t) \quad (26\text{–}1)$$

$$y_2 = C_2 x_2(t) + \nu_2(t) \quad (26\text{–}2)$$

Where, $x_2 \in$ ^{6} is system state with the following parameters:

$$x_2 = \begin{bmatrix} b_{0q_2} & b_{1q_2} & s_{fq_2} & b_{0p_3} & b_{1p_3} & s_{fp_3} \end{bmatrix}^T \quad (27)$$

And, $y_2[S_{m_{q_2}} \; S_{m_{p3}}]^T \in$ ^{2} is system output which shows the sensor measurements. $\omega_2(t)$ and $\nu_2(t)$ are process and measurement noises. Besides:

$$A_2 = \text{diag}(0, -1/\tau_{q_2}, 0, 0, -1/\tau_{p_3}, 0) \quad (28)$$

$$C_2 = \begin{bmatrix} 1 & 1 & q_2 & 0 & 0 & 0 \\ 0 & 0 & 0 & 1 & 1 & p_3 \end{bmatrix} \quad (29)$$

Augmenting, pump and sensory soft fault models, the following continuous time linear model is obtained:

$$\dot{x}'_T(t) = A'_T x'_T(t) + B'_T u(t) + \omega'_T(t) \quad (30\text{–}1)$$

$$y'_T = C'_T x'_T(t) + \nu'_T(t) \quad (30\text{–}2)$$

Where, $x'_T \in$ ^{11} is system state with the following parameters:

$$x'_T = [q_1 \;\; q_2 \;\; p_2 \;\; p_3 \;\; p_4 \;\; b_{0q_2} \;\; b_{1q_2} \;\; s_{fq_2} \;\; b_{0p_3} \;\; b_{1p_3} \;\; s_{fp_3}]^T \quad (31)$$

$u'_T \in$ ^{1} is system input:

$$u'_T = p_s \quad (32)$$

And, $y'_T \in$ ^{2} is system output which shows the sensor measurements. $\omega(t)$ and $\nu(t)$ are process and measurement noises with Gaussian probability distribution.

$$A'_T = \begin{bmatrix} A'_{11} & 0 \\ 0 & A'_{22} \end{bmatrix}_{11\times 11} \quad (33)$$

$$A'_{11} = \begin{bmatrix} \frac{-(R_1+R_2)}{L_1} & \frac{R_3+L_2}{L_1L_3} & 0 & -\frac{1}{L_1}(1+\frac{L2}{L3}) & \frac{L_2}{L_1L_3} \\ \frac{-R_2}{L_2} & 0 & \frac{1}{L_2} & -\frac{1}{L_2} & 0 \\ \frac{1}{C_1}+\frac{L_3}{C_1L_2}-\frac{R_2(R_1+R_2)}{L_2} & -\frac{1}{C_1}+\frac{1}{C_2}-\frac{L_3}{C_1L_2}+\frac{R_3^2}{L_3}+\frac{R_2R_3L_2}{L_1L_3} & 0 & \frac{-R_3}{L_3}-\frac{R_2}{L_1}(1+\frac{L_2}{L_3}) & \frac{R_3}{L_3}-\frac{1}{RC_2}+\frac{R_2L_2}{L_1L_3} \\ \frac{L_3}{C_1L_2} & \frac{1}{C_2}-\frac{L_3}{C_1L_2}+\frac{R_3^2}{L_3} & 0 & -\frac{R_3}{L_3} & \frac{R_3}{L_3}-\frac{1}{RC_2} \\ 0 & \frac{1}{C_2} & 0 & 0 & -\frac{1}{RC_2} \end{bmatrix}$$

And $A'_{22} = A_2$ is defined in Equation (28) and other parameters are defined in Section 2.2. Besides,

$$C'_T = \begin{bmatrix} 0 & 1 & 0 & 0 & 0 & 1 & 1 & q_2 & 0 & 0 & 0 \\ 0 & 0 & 0 & 1 & 0 & 0 & 0 & 0 & 1 & 1 & p_3 \end{bmatrix} \quad (34)$$

Discretizing the state space model, the following is obtained:

$$x'_{T,k+1} = \varphi'_T x'_{T,k} + \Gamma'_T u'_T(k) + \omega'_{T,k} \quad (35)$$

Where $x'_{T,k}$ is the state vector of the process at time instant k, φ'_T is the state transition matrix of the process from the state at k k to state at $k+1$, $\omega'_{T,k}$ is the associated discrete zero mean white Gaussian noise with the known covariance matrix of $Q'_T = E[\omega'_{T,k}\omega'_{T,k}{}^T]$. Observations on this variable can be modeled in the form;

$$y'_{T,k} = H'_T x'_{T,k} + \nu'_{T,k} \quad (36)$$

Where; $y'_{T,k}$ is the sensor measurement model H'_T is the measurement vector, $\nu'_{T,k}$ is the discrete measurement zero mean white Gaussian noise with the known covariance matrix of $R'_T = E[\nu'_{T,k}\nu'_{T,k}{}^T]$. This is again assumed to be a white noise process with known covariance and has zero cross-correlation with the process noise.

4. SIMULATION RESULTS

In this part of article, simulation results are provided to demonstrate the effectiveness of our proposed method. To this purpose, Extended Kalman filtering (EKF) ([25]) is employed to the system introduced in Section 3. Values of the model parameters in our simulation are summarized in Table 1.

Table 1. Kalman Filter Recursive Algorithm.

Parameter	Values	Parameter	Values
R_s	10.9Ω	p	2
R_r	20.69Ω	J	0.089
L_s	$1H$	L_1	$0.5m$
L_r	$3H$	L_2	$1m$
L_M	$0.007857H$	L_3	$1m$
g	$9.8m/s^2$	s	$\pi*0.5^2m^2$
ρ	0.00001	A	$\pi*0.1^2m^2$
R	$1lit/(\min*bar)$	$\tau_{i_\alpha}, \tau_{i_\beta}$	$300s$
R_1, R_2, R_3	$30\ \Omega$	τ_{q_2}, τ_{P_3}	$10s$

System and measurement noise parameters for motor and pump are selected as follows:

$$Q_T = Q'_T =$$
$$\text{diag}(5\times10^{-3}, 8\times10^{-3}, 5\times10^{-3}, 8\times10^{-3}, 5\times10^{-3}, 10^{-7}, 10^{-2}, 10^{-7}, 10^{-7}, 10^{-2}, 10^{-7})$$
$$R_T = \text{diag}(0.02, 0.0225, 0.02)$$
$$R'_T = 10^{-4} \times \text{diag}(1,1)$$

Fig. 7 Estimations the system state estimate compared to real (simulated) values for engine modeling. Appraisal of sensory soft faults compared to the true values are indicated in Fig. 8.

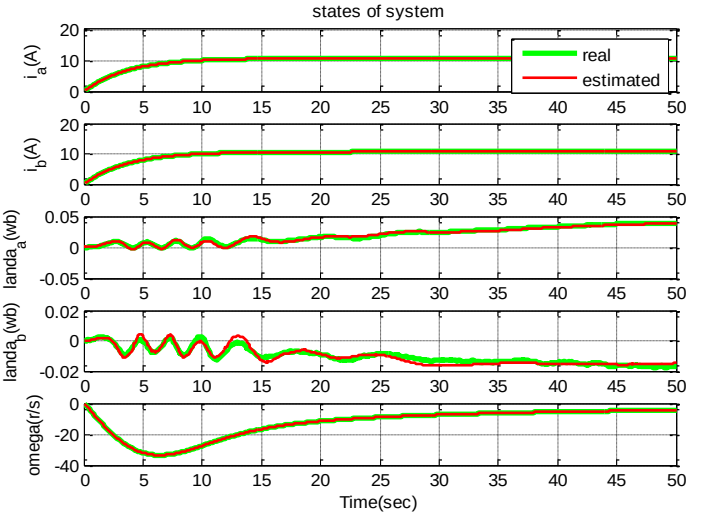

Fig. 7. Appraisal of states of The motor system: $i_\alpha, i_\beta, \lambda_\alpha, \lambda_\beta, \omega$.

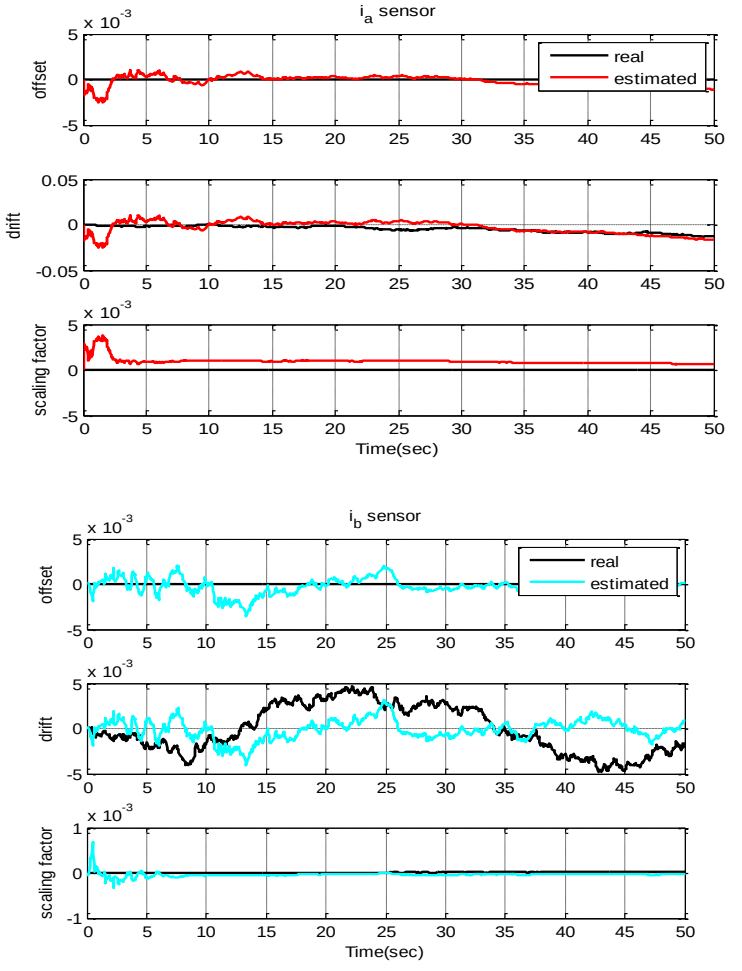

Fig. 8. Estimation of sensor faults (bias , drift, and scaling factor terms for two current sensors).

Fig. 9 Demonstrates evaluations of the state of the system compared to the actual simulated values for pump modeling. Appraisal of sensory soft errors compared to actual values is indicated in Fig. 10.

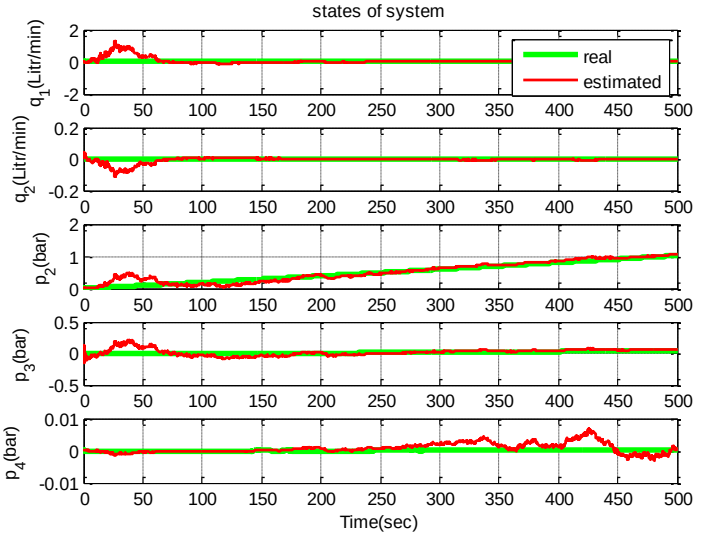

Fig. 9. Estimation of states of the pump system: q_1, q_2, p_2, p_3, p_4.

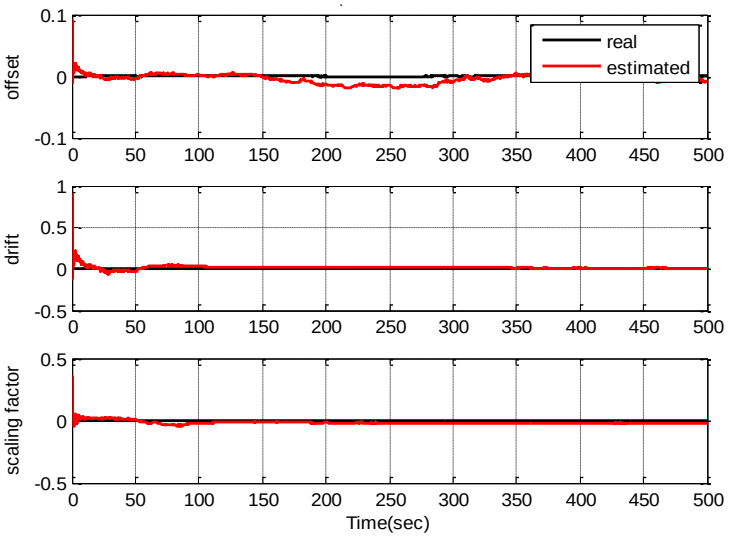

(a) Flow sensor

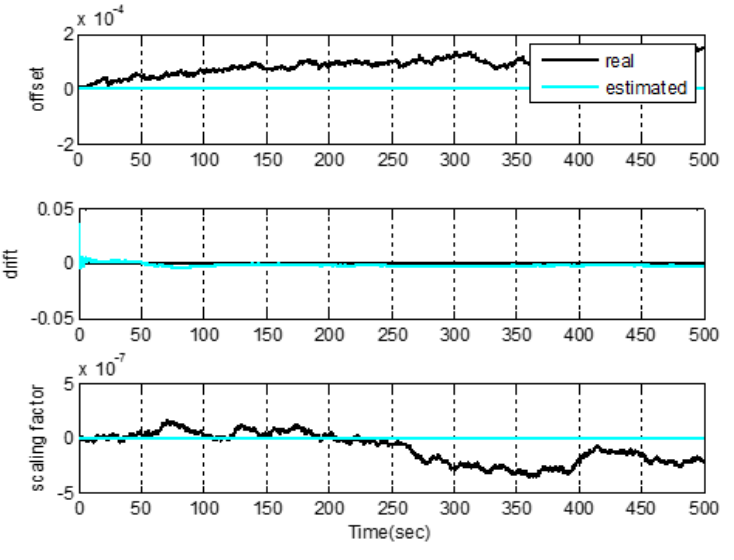

(b) Pressure sensor

Fig. 10. Estimation of sensor faults (bias ,drift and scaling factor terms for and pressure sensors).

5. EXPERIMENTAL RESULTS

In this section, experimental results are provided to demonstrate the effectiveness of our proposed method. The employed experimental setup is depicted in Fig. 2. Data is transferred to a computer via an ADVANTECH PCI-1711 data card with the minimum frequency of 10^{-4} Hz. Fig. 11 and Fig. 12. depict the results.

Because of providing a scalar assessment for the prediction performance, the Root Mean Square Error (RMSE) was used. It is formulated as follows:

$$RMSE = \sqrt{\frac{1}{N}\sum_{k=1}^{N} e(k)^T e(k)} \tag{37}$$

Which $e(k) = x(k) - \hat{x}(k)$, N indicates the total number of parables. The RMSE is obtained for one round algorithm implemented in Table 2.

Which refers to the total number of samples. The RMSE is obtained for a round algorithm implemented in Table 2.

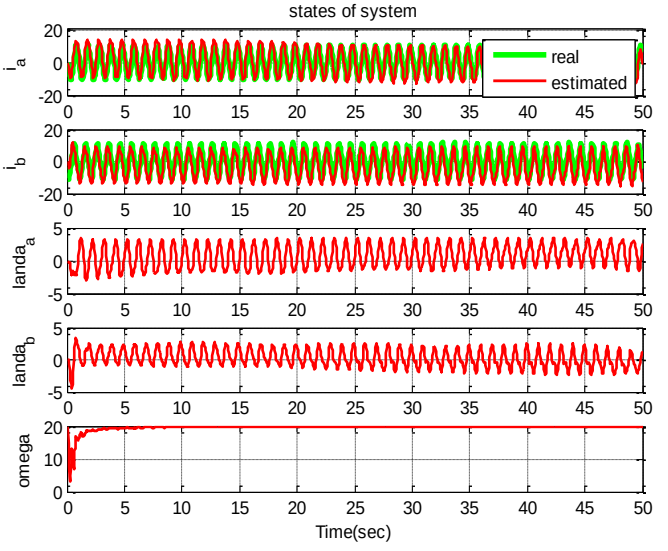

Fig. 11. Estimation of sensor faults (bias ,drift and scaling factor terms for and pressure sensors).

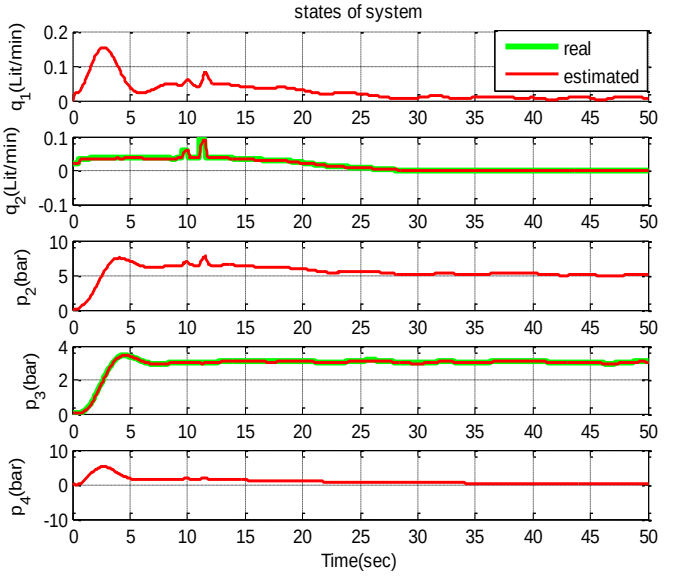

Fig. 12. Estimation of sensor faults (bias, drift and scaling factor terms for and pressure sensors).

Table 2. The RMSE values for simulation data.

System	RMSE
motor	0.0024
pump	0.0247
motor with sensor faults	0.0058
pump with sensor faults	0.0581

6. CONCLUSIONS

In this article, a fault identification and detection method for evaluating system states and soft sensory faults is presented simultaneously. For this purpose, we first proposed a mathematical model for the pump system using the electrical analogy method. Then, soft sensory faults including biases, drifts and scaling factors were modeled and added to the system state space model. The nonlinear model of the induction motor was linearized for use in the Extended Kalman filter. Ultimately, the method was appraised simulation and experimental data.

REFERENCES

[1] Dutta N, Palanisamy K, Subramaniam U, Padmanaban S, Holm-Nielsen JB, Blaabjerg F, Almakhles DJ**. "Identification of Water Hammering for Centrifugal Pump Drive Systems".** *Applied Sciences*. 2020 Jan;10(8), 2683.

[2] P. Samanipour and J. Poshtan, "**Electro pump modeling using laboratory system data,"** in *Power Electronics and Drive Systems Technologies Conference (PEDSTC), 2016 7th*, 2016, pp. 111-115.

[3] N. S. Nokhodberiz and J. Poshtan, **"Belief consensus–based distributed particle filters for fault diagnosis of non-linear distributed systems,"** *Journal of Systems and Control Engineering*, Vol. 228, No.3, pp. 123-137, 2013..

[4] S. Mondal, G. Chakraborty, and K. Bhattacharyy, **"LMI approach to robust unknown input observer design for continuous systems with noise and uncertainties,"** *International Journal of Control, Automation and Systems*, Vol. 8, pp. 210-219, 2010.

[5] V. F. Pires, J. Martins, and A. Pires, **"Eigenvector/eigenvalue analysis of a 3D current referential fault detection and diagnosis of an induction motor,"** *Energy conversion and management*, Vol. 51, pp. 901-907, 2010.

[6] A. Lemos, W. Caminhas, and F. Gomide, **"Adaptive fault detection and diagnosis using an evolving fuzzy classifier,"** *Information Sciences*, Vol. 220, pp. 64-85, 2013.

[7] H. Jafari and J. Poshtan, **"Fault isolation and diagnosis of induction motor based on multi-sensor data fusion,"** in *Power Electronics, Drives Systems & Technologies Conference (PEDSTC), 2015 6th*, 2015, pp. 269-274.

[8] Z. Tian, L. Wong, and N. Safaei, **"A neural network approach for remaining useful life prediction utilizing both failure and suspension histories,"** *Mechanical Systems and Signal Processing*, Vol. 24, pp. 1542-1555, 2010.

[9] N. Sakthivel, V. Sugumaran, and S. Babudevasenapati, **"Vibration based fault diagnosis of monoblock centrifugal pump using decision tree,"** *Expert Systems with Applications*, Vol. 37, pp. 4040-4049, 2010.

[10] Manohar M, Das S. **"Current sensor fault-tolerant control of induction motor driven electric vehicle using flux-linkage observer"**. *In2020 IEEE Transportation Electrification Conference & Expo (ITEC) 2020 Jun 23 (pp. 884-889)*. IEEE.

[11] J. Alonso, M. Ferrer, and C. Travieso, **"Fault diagnosis using audio and vibration signals in a circulating pump,"** in *Journal of Physics: Conference Series*, 2012, p. 012135.

[12] Rkhissi-Kammoun Y, Ghommam J, Boukhnifer M, Mnif F. **"Two current sensor fault detection and isolation schemes for induction motor drives using algebraic estimation approach"**. *Mathematics and Computers in Simulation*. Mar 1;157, pp. 39-62, 2019.

[13] N. Sadaghzadeh N. J. Poshtan, A. Wagner, E. Nordheimer, and E. Badreddin, **"Cascaded Kalman and particle filters for photogrammetry based gyroscope drift and robot attitude estimation,"** *ISA transactions*, Vol. 53, pp. 524-532, 2014.

[14] F. Aguilera, M. Pablo, and C. H. De Angelo, **"Behavior of electric vehicles and traction drives during sensor faults,"** in *Industry Applications (INDUSCON), 2012 10th IEEE/IAS International Conference on*, 2012, pp. 1-7.

[15] S. K. Kommuri, J. J. Rath, K. C. Veluvolu, M. Defoort, and Y. C. Soh, **"Decoupled current control and sensor fault detection with second-order sliding mode for induction motor,"** *IET Control Theory & Applications*, Vol. 9, pp. 608-617, 2015.

[16] A. Raisemche, M. Boukhnifer, C. Larouci, and D. Diallo, "**Two active fault-tolerant control schemes of induction-motor drive in EV or HEV,"** *IEEE Transactions on Vehicular Technology*, Vol. 63, pp. 19-29, 2014.

[17] X. Shi and M. Krishnamurthy, **"Survivable operation of induction machine drives with smooth transition strategy for EV applications,"** *IEEE Journal of Emerging and Selected Topics in Power Electronics*, Vol. 2, pp. 609-617, 2014.

[18] N. M. Freire, J. O. Estima, and A. J. M. Cardoso, **"A new approach for current sensor fault diagnosis in PMSG drives for wind energy conversion systems,"** *IEEE Transactions on Industry Applications*, Vol. 50, pp. 1206-1214, 2014.

[19] X. Zhang, G. Foo, M. D. Vilathgamuwa, K. J. Tseng, B. S. Bhangu, and C. Gajanayake, **"Sensor fault detection, isolation and system reconfiguration based on extended Kalman filter for induction motor drives,"** *IET Electric Power Applications*, Vol. 7, pp. 607-617, 2013.

[20] T. A. Najafabadi, F. R. Salmasi, and P. Jabehdar-Maralani, **"Detection and isolation of speed-, DC-link voltage-, and current-sensor faults based on an adaptive observer in induction-motor drives,"** *IEEE Transactions on Industrial Electronics*, Vol. 58, pp. 1662-1672, 2011.

[21] F. Aguilera, P. de la Barrera, C. De Angelo, and D. E. Trejo, "**Current-sensor fault detection and isolation for induction-motor drives using a geometric approach,"** *Control Engineering Practice*, Vol. 53, pp. 35-46, 2016.

[22] N. Sadeghzadeh-Nokhodberiz, J. Poshtan, A. Wagner, E. Nordheimer, and E. Badreddin, **"Distributed observers for pose estimation in the presence of inertial sensory soft faults,"** *ISA transactions*, Vol. 53, pp. 1307-1319, 2014.

[23] M. Sepasi, **"Fault monitoring in hydraulic systems using unscented Kalman filter,"** *University of British Columbia*, 2007.

[24] D. Gebre-Egziabher, "**Design and performance analysis of a low-cost aided dead reckoning navigator,"** *Citeseer*, 2004.

[25] G. Welch and G. Bishop, **"An introduction to the kalman filter. Department of Computer Science, University of North Carolina,"** *ed: Chapel Hill, NC, unpublished manuscript*, 2006.